



Research paper

Endoperoxide-8-aminoquinoline hybrids as dual-stage antimalarial agents with enhanced metabolic stability

Rita Capela ^{a,1}, Joana Magalhães ^{a,1}, Daniela Miranda ^{a,1}, Marta Machado ^b, Margarida Sanches-Vaz ^b, Inês S. Albuquerque ^b, Moni Sharma ^a, Jiri Gut ^c, Philip J. Rosenthal ^c, Raquel Frade ^a, Maria J. Perry ^a, Rui Moreira ^a, Miguel Prudêncio ^{b,**}, Francisca Lopes ^{a,*}

^a Instituto de Investigação do Medicamento (iMed.Ulisboa), Faculdade de Farmácia, Universidade de Lisboa, Av. Prof. Gama Pinto, 1649-003 Lisboa, Portugal

^b Instituto de Medicina Molecular, Faculdade de Medicina, Universidade de Lisboa, Av. Professor Egas Moniz, 1649-028, Lisboa, Portugal

^c Department of Medicine, San Francisco General Hospital, University of California, San Francisco, Box 0811, CA 94143, USA

ARTICLE INFO

Article history:

Received 8 November 2017

Received in revised form

28 January 2018

Accepted 14 February 2018

Available online 19 February 2018

Keywords:

Malaria

Hybrid drugs

Liver stage

Dual-stage antimalarials

Metabolism

ABSTRACT

Hybrid compounds may play a critical role in the context of the malaria eradication agenda, which will benefit from therapeutic tools active against the symptomatic erythrocytic stage of *Plasmodium* infection, and also capable of eliminating liver stage parasites. To address the need for efficient multistage antiplasmodial compounds, a small library of 1,2,4,5-tetraoxane-8- aminoquinoline hybrids, with the metabolically labile C-5 position of the 8-aminoquinoline moiety blocked with aryl groups, was synthesized and screened for antiplasmodial activity and metabolic stability. The hybrid compounds inhibited development of intra-erythrocytic forms of the multidrug-resistant *Plasmodium falciparum* W2 strain, with EC₅₀ values in the nM range, and with low cytotoxicity against mammalian cells. The compounds also inhibited the development of *P. berghei* liver stage parasites, with the most potent compounds displaying EC₅₀ values in the low μM range. SAR analysis revealed that unbranched linkers between the endoperoxide and 8-aminoquinoline pharmacophores are most beneficial for dual antiplasmodial activity. Importantly, hybrids were significantly more potent than a 1:1 mixture of 8-aminoquinoline-tetraoxane, highlighting the superiority of the hybrid approach over the combination therapy. Furthermore, aryl substituents at C-5 of the 8-aminoquinoline moiety improve the compounds' metabolic stability when compared with their primaquine (i.e. C-5 unsubstituted) counterparts. Overall, this study reveals that blocking the quinoline C-5 position does not result in loss of dual-stage antimalarial activity, and that tetraoxane-8- aminoquinoline hybrids are an attractive approach to achieve elimination of exo- and intraerythrocytic parasites, thus with the potential to be used in malaria eradication campaigns.

© 2018 Elsevier Masson SAS. All rights reserved.

1. Introduction

Malaria is a major global public health problem, with 214 million new clinical cases and 440,000 deaths estimated in 2015 [1]. The disease is caused by *Plasmodium* parasites, with *P. falciparum* and *P. vivax* causing the heaviest burden. *P. falciparum*

is responsible for most malaria-associated mortality, while *P. vivax* can generate cryptic parasite forms called hypnozoites that persist in the liver for long periods of time, causing relapsing malaria [2–4]. The life cycles of all *Plasmodium* spp. also include a liver stage that precedes erythrocytic infection and a sexual blood form, the gametocyte, that is responsible for transmission from the mammalian host to the mosquito vector [5]. There is an urgent need for efficacious and safe tools for malaria prophylaxis and to effectively prevent the relapse of *P. vivax* malaria, as well as to treat and block the transmission of the disease [6–8]. Despite increasing efforts worldwide, available compounds active against non-erythrocytic stages of malaria parasites remain very limited [3].

* Corresponding author.

** Corresponding author.

E-mail addresses: mprudencio@medicina.ulisboa.pt (M. Prudêncio), fclopes@ff.ulisboa.pt (F. Lopes).

¹ These authors contributed equally to this work.

Primaquine, **1** (Fig. 1), is the only licensed drug active against *P. vivax* hypnozoites, and is thus used for radical cure of infections by this parasite [3,9]. In addition, primaquine is the only available antimalarial agent that displays marked activity against gametocytes from all species of parasites causing human malaria, and is therefore capable of interrupting disease transmission from the host to the mosquito vector [9]. However, primaquine's clinical value is compromised by its toxic side effects, namely methaemoglobinaemia and hemolytic anemia in patients with deficiency in glucose-6-phosphate dehydrogenase (G6PD) activity [9]. The methaemoglobinaemia associated with primaquine is thought to be a consequence of cytochrome P450-mediated oxidation of the corresponding 5-hydroxylated metabolites to quinoneimine [9,10].

Currently, WHO recommends the use of artemisinin-based combination therapies (ACTs) as first line treatment for uncomplicated malaria [11]. However, increasing resistance to ACTs, due to decreased activity of both artemisinins and partner drugs, has been reported in Southeast Asia, and spread of resistance to other regions may have devastating consequences [12–16].

Hybrid compounds capable of hitting more than one molecular target are an attractive alternative to ACTs [17–23]. Such compounds may be particularly relevant in the context of the malaria eradication agenda, which benefits from therapeutic tools not only active against the symptomatic erythrocytic stage of infection, but also capable of eliminating liver-stages and/or gametocytes [8,24]. In this context, we recently reported new peroxide-based hybrid compounds comprising a primaquine moiety combined with an endoperoxide pharmacophore, e.g. **2** (artemisinin-based) and **3** (1,2,4,5-tetraoxane-based), that showed high potency against both liver and blood stages of malaria parasites [25,26]. In addition, hybrid **3** also blocked transmission to the mosquito in an animal model. However, the most potent compounds displayed high metabolic susceptibility in rat liver microsomes, dependent on the nature of the linker between the tetraoxane and primaquine moieties [26].

Here, we report the design, synthesis and antiplasmodial activity of tetraoxane-8-aminoquinoline hybrids, **4** (Fig. 1), with an aryl or heteroaryl group installed at the metabolically labile C-5 position of the 8-aminoquinoline moiety. 5-Hydroxy-8-aminoquinolines are thought to be the metabolites responsible for the hemolytic toxicity associated with primaquine and other 8-aminoquinolines, and thus blocking C-5 offers the potential to resolve the toxicity liability [9,27]. 5-Aryl-8-aminoquinolines, designed to probe the possibility of separating antimalarial activity

from hemolytic toxicity in 8-aminoquinolines, have been reported to be metabolically stable, but inactive against the exoerythrocytic mouse model, with moderate activity against intraerythrocytic parasites [28]. We now report that tetraoxane-8-aminoquinoline hybrids, **4**, are metabolically more stable than their primaquine counterparts, **3**, while retaining activity against liver stage parasites.

2. Results and discussion

2.1. Chemistry

The library of tetraoxane-8-aminoquinoline hybrids was prepared based on a synthetic procedure involving the following steps: (i) synthesis of a C-5 substituted 8-aminoquinoline key intermediate, (ii) incorporation of a diamine spacer, and (iii) coupling to the appropriately functionalized tetraoxane (**4**, Fig. 1).

The preparative route for the C-5 substituted 8-aminoquinoline intermediate, **5** (Scheme 1), was an adaptation from that described by Chen [29] and Shiraki et al. [28] First, bromination of the commercially available 6-methoxy-8-nitroquinoline, **6**, was achieved using bromine and Fe (Scheme 1). The resulting 5-bromo-6-methoxy-8-nitroquinoline **7** was then converted to the appropriate 5-aryl-6-methoxy-8-nitroquinolines, **8**, in satisfactory yields by Suzuki coupling reactions with a series of arylboronic acids using Pd(OAc)₂, PPh₃ and Na₂CO₃ in dimethoxyethane. Finally, reduction of **8** using Sn/SnCl₂ [30] gave the intermediates **5** in 76% overall yield.

Scheme 2 outlines the general route to incorporate the diamine spacer into intermediate **5**, which was adapted from Elderfield et al. [31] First, reaction of phthalimide potassium salt, **10**, with the appropriate dibromoalkane afforded the corresponding bromoalkylphthalimide intermediates **11a-d**. Reaction of intermediates **5a-h** with **11a-d** gave moderate to excellent yields of the desired **12a-l**, which were then converted to the corresponding amines **13a-l** by hydrazinolysis.

In the development of hybrids **4**, we explored the nature of the chemical group between the tetraoxane moiety and the linker. Amide derivatives, **4a-l**, were prepared by reacting tetraoxane **14** [22] with intermediates **13a-l**, using TBTU as coupling agent, while their amine counterparts, **4m-s**, were synthesized by reductive amination of tetraoxane **15** [26] with **13a-h** and NaBH(AcO)₃ (Scheme 3). Finally, hybrid compounds **16a-d**, which do not contain any linker between the tetraoxane and 8-aminoquinoline moieties,

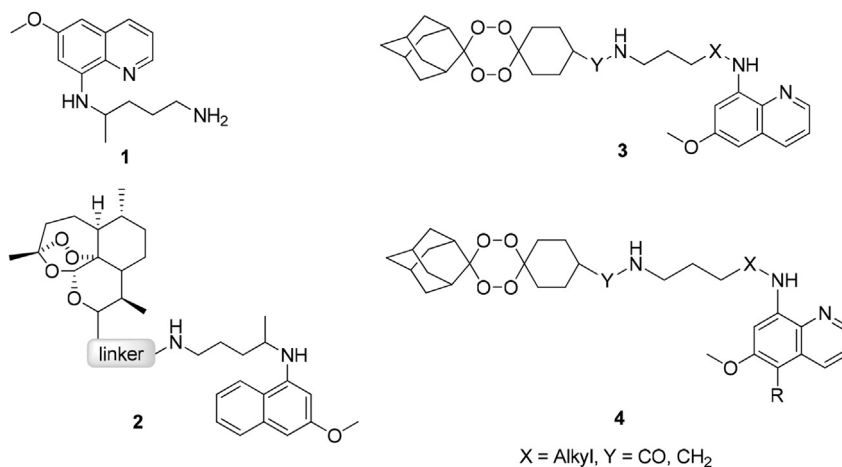
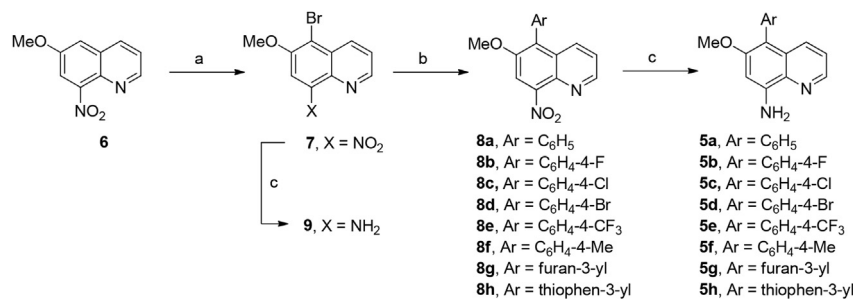
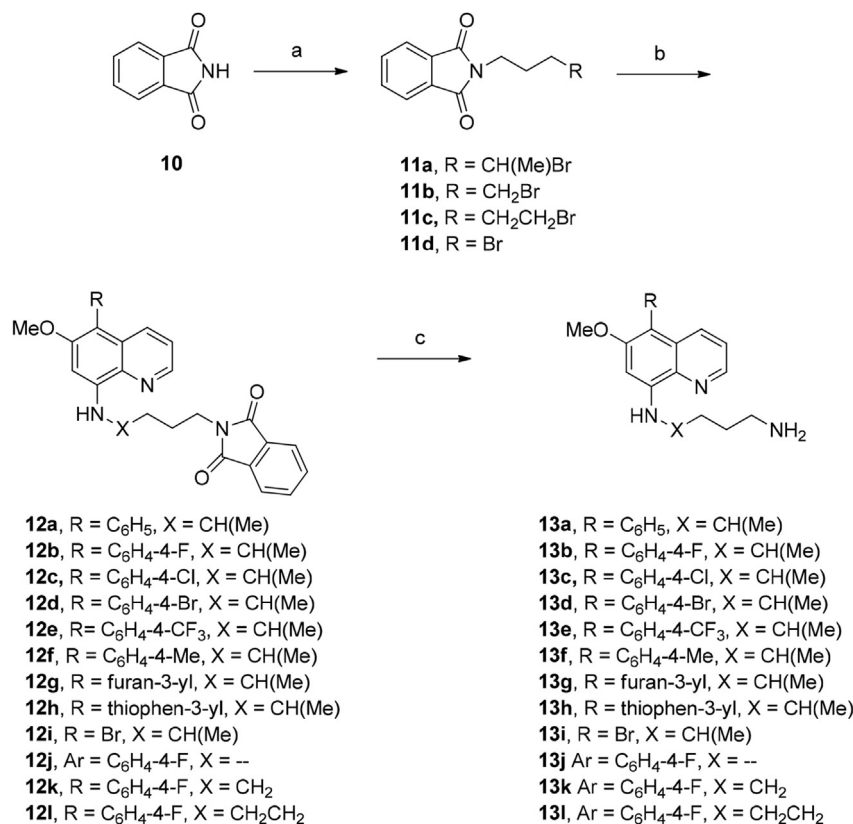


Fig. 1. Chemical structures of primaquine **1**, artemisinin-based hybrids **2**, 1,2,4,5-tetraoxane-primaquine hybrids **3**, and 1,2,4,5-tetraoxane-8-aminoquinoline hybrids reported in this study, **4**.

**Scheme 1.** Synthesis of compounds 5 and 7-9^a.^aReagents and conditions: (a) Br₂, Fe, CaCO₃, DCM, H₂O, reflux 15 h, then rt 6 h; (b) Pd(OAc)₂, PPh₃, Na₂CO₃, TBAB, ArB(OH)₂, dimethoxyethane, reflux; (c) Sn, SnCl₂, HCl, 0 °C.**Scheme 2.** Synthesis of intermediates 11-13^a.^aReagents and conditions: (a) 1) KOH, EtOH, reflux, 2) dibromoalkane, acetone, reflux 24 h; (b) **5a-h** or **9**, TEA, reflux, 19 h; (c) NH₂NH₂, EtOH, reflux 7 h.

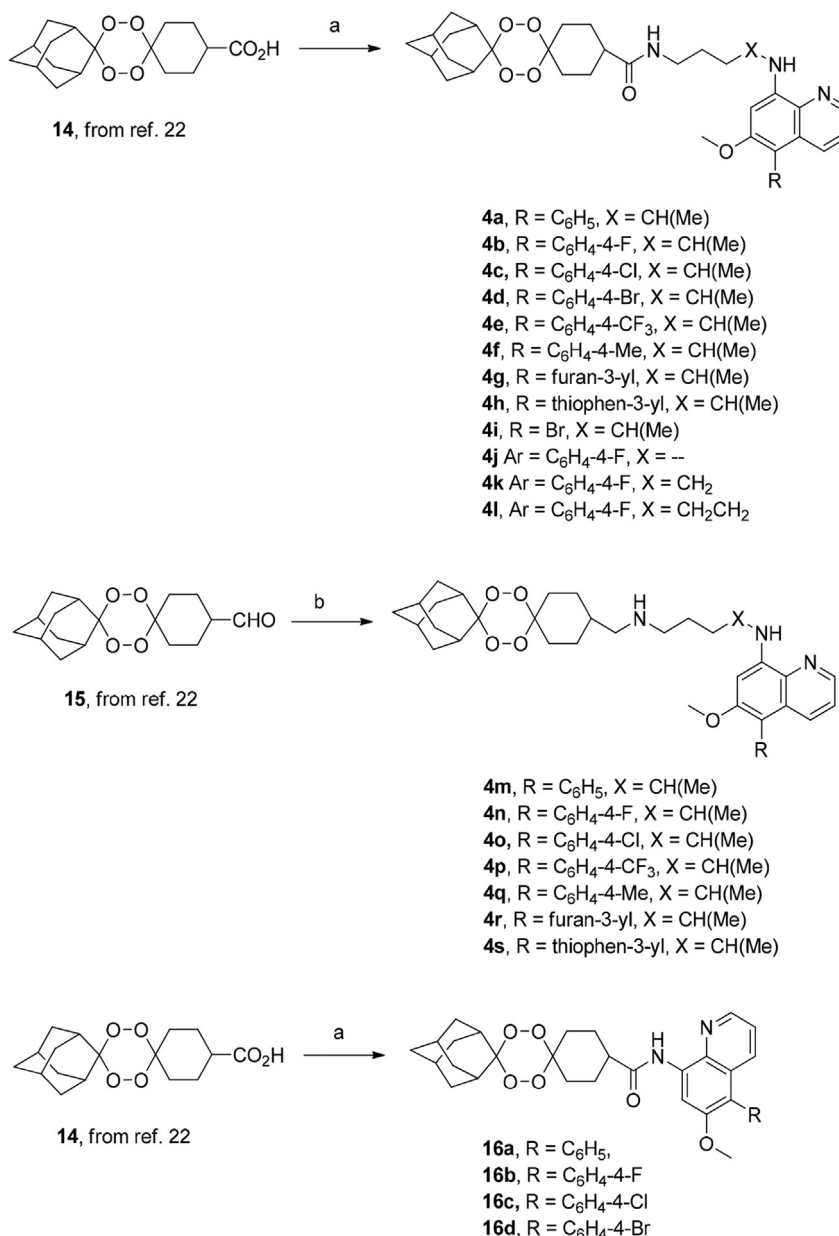
were prepared by reacting the appropriate 8-aminoquinoline **16** with intermediate **14** previously activated with ethyl chloroformate.

2.2. Blood schizontocidal activity and cytotoxicity

Compounds **4** and **16** were first screened for activity against intraerythrocytic parasites, using cultured chloroquine-resistant W2 strain *P. falciparum*; the corresponding EC₅₀ values are presented in Table 1. EC₅₀ values for **4a-s** ranged from 15 to 200 nM, in line with the values previously reported for their primaquine counterparts (e.g. **3a**, EC₅₀ 21 nM, Table 1) [26]. This result contrasted sharply with that for derivatives **16a-d**, which lack a linker between the endoperoxide and 8-aminoquinoline moieties. These compounds were ca. 10 to 50 times less potent than their counterparts **4** (e.g. **4b** or **4j** versus **16b** or **4d** versus **16d**), suggesting

that the presence of a linker is a major requirement for activity against intraerythrocytic parasites.

Structure-activity relationship studies indicated that the blood-schizontocidal activity of hybrids **4a-s** was affected by the nature of the linker between the endoperoxide and 8-aminoquinoline moieties as well as by the substituent on the C-5 position of the quinoline moiety. For example, compounds containing linear linkers (**4j-l**) generally presented better antiplasmodial activity than those with branched linkers (e.g. **4b**). In contrast, the basicity of the linker nitrogen atom close to the endoperoxide moiety had limited impact on blood-stage activity, as shown by the EC₅₀ values for the amide series, **4a-h**, when compared to those of their amine counterparts, **4m-s**. The electronic effects of the substituent at the C-5 position of the quinoline moiety also influenced inhibitory activity against erythrocytic parasites. For the amide series, **4a-i**, compounds containing electron withdrawing groups (e.g. 4-Br, **4i**,



Scheme 3. Synthesis of hybrids **4** and **16**^a.

^aReagents and conditions: (a) 1) TBUT, DCM, TEA, 0 °C, 1 h, 2) **13a-l** for **4a-l** or **5a-d** for **16a-d**, DCM, TEA, rt.; (b) DCM, **13a-c** and **13e-h** for **4m-s**, AcOH, STAB, rt.

$\sigma_p = 0.22$ [32], or 4-fluorophenyl, **4b**, $\sigma_p = 0.06$ [32]) showed better activity than those with electron donating substituents (e.g. 4-methylphenyl, **4f**, $\sigma_p = -0.05$ [32]). The exception was compound **4h**, containing the electron-rich 3-thienyl substituent at C-5 ($\sigma_p = -0.02$ [32]), which also displayed excellent blood-stage activity.

The *in vitro* cytotoxicity of compounds **4** was evaluated using mammalian CaCo-2 cells (Table 1). The selectivity index (SI) as expressed by the ratio $CC_{50}^{CaCo-2}/IC_{50}^{W2}$, ranged from ca. 60 to >1000, with compounds **4b-e** and **4g,h** displaying the highest CC_{50} and SI values (>50 and > 600, respectively).

2.3. Liver schizontocidal activity

Hybrid derivatives **4** and **16** were further evaluated for their ability to inhibit the development of liver-stage malaria parasites.

Compounds were initially assayed at two different concentrations (2 and 10 μ M), using an *in vitro* infection model that employs a human hepatoma cell line (Huh7) infected with firefly luciferase-expressing *P. berghei*. Results were compared to those obtained for primaquine (Fig. 2). Strikingly, hybrids with an amide linker between the two pharmacophores, **4a-l**, were highly active, with >50% inhibition of infection at 2 μ M, and almost complete suppression at 10 μ M, without significantly affecting Huh7 cell proliferation. The exception was the 5-bromo derivative **4i**, which was toxic to Huh7 cells at 10 μ M. In contrast, derivatives with an amine linker, i.e. **4m-s**, inhibited infection at both concentrations, but showed toxicity towards host Huh7 cells at 10 μ M. Finally, hybrids lacking a linker between the two pharmacophores, **16a-d**, did not demonstrate significant liver stage activity, indicating that the presence of a linker is required to convey potency against liver stage parasites.

Table 1

In vitro antimalarial activities (EC₅₀) against intraerythrocytic *P. falciparum* W2 strain and liver-stage *P. berghei*, and toxicity (CC₅₀) of hybrid compounds **4** and **16** against CaCo-2 cells.

Compd	Y	X	R	EC ₅₀ /μM		CC ₅₀ /μM	Compd	Y	X	R	EC ₅₀ /μM		CC ₅₀ /μM
				<i>P. falciparum</i> W2 (blood stage)	<i>P. berghei</i> (liver stage)						<i>P. falciparum</i> W2 (blood stage)	<i>P. berghei</i> (liver stage)	
4a	CO	CH(Me)		0.204 ± 0.013	1.69 ± 0.33	>50	4m	CH ₂	CH(Me)		0.092 ± 0.007	Tox.	ND
4b	CO	CH(Me)		0.057 ± 0.012	2.38 ± 0.56	>50	4n	CH ₂	CH(Me)		0.099 ± 0.004	ND	ND
4c	CO	CH(Me)		0.075 ± 0.002	2.81 ± 0.56	>50	4o	CH ₂	CH(Me)		ND	Tox.	13.2
4d	CO	CH(Me)		0.061 ± 0.020	4.44 ± 0.66	>50	4p	CH ₂	CH(Me)		0.019 ± 0.003	62% ^a inhib at 10 μM	10.3
4e	CO	CH(Me)		0.060 ± 0.009	4.12 ± 0.49	>50	4q	CH ₂	CH(Me)		0.176 ± 0.009	Tox.	11.7
4f	CO	CH(Me)		0.141 ± 0.021	1.65 ± 0.53	>50	4r	CH ₂	CH(Me)		0.120 ± 0.005	ND	ND
4g	CO	CH(Me)		0.076 ± 0.010	2.35 ± 0.19	>50	4s	CH ₂	CH(Me)		0.081 ± 0.003	Tox.	ND
4h	CO	CH(Me)		0.045 ± 0.002	2.11 ± 0.13	>50	16a	CO	–		0.287 ± 0.015	52% ^a inhib at 10 μM	ND
4i	CO	CH(Me)	Br	0.016 ± 0.004	Tox.	ND	16b	CO	–		0.916 ± 0.047	ND	ND
4j	CO	–		0.015 ± 0.003	2.61 ± 0.08	ND	16c	CO	–		4.19 ± 0.20	37% ^a inhib at 10 μM	ND
4k	CO	CH ₂		0.015 ± 0.005	1.11 ± 0.40	10.2	16d	CO	–		5.67 ± 0.43	35% ^a inhib at 10 μM	ND
4l	CO	CH ₂ CH ₂		0.017 ± 0.003	1.64 ± 0.15	ND	13f	–	CH(Me)		2.35 ± 0.07	5.43 ± 1.17	ND
ART				0.010 ± 0.001	ND	ND	3a	CO	CH(Me)	H	0.021 [26]	0.538 [26]	ND
PQ				ND	7.50 [26]	ND	PQ + ART				ND	9.71 [26]	ND
14 ethyl ester				128.2 [26]	17.3 ± 3.9	ND	13f–14 ester				ND	3.71 ± 0.32	ND

^a Percentage of inhibition at 10 μM; ND: Not determined; Tox: toxic to the host cells.

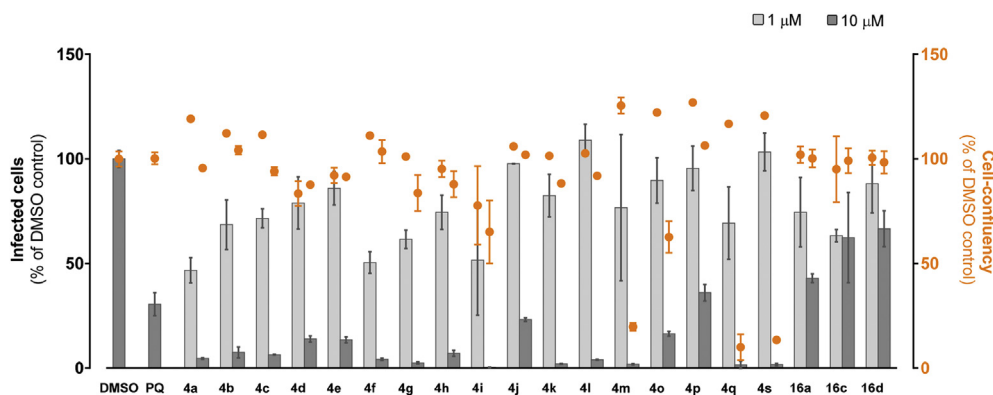


Fig. 2. Hybrid compounds **4** and **16** inhibit the development of *Plasmodium* hepatic stages *in vitro* to different extents. Huh7 cells were infected with luciferase-expressing *P. berghei* sporozoites and treated with 1 and 10 μM of each hybrid compound or with equivalent amounts of dimethyl sulfoxide (DMSO; control). Primaquine (PQ) was used as a positive control. Total parasite loads (bioluminescence) and cell viability (AlamarBlue fluorescence) were assessed at 48 h post infection. Bars represent infection and dots represent Huh7 cell confluency. Error bars represent standard deviation.

Based on these observations, we then determined EC₅₀ values for the amide derivatives, **4a–h** and **4j–l**, against *P. berghei* infection of Huh7 cells. These compounds presented EC₅₀ values ranging from 1.1 to 4.3 μM for inhibition of hepatic infection, compared to 0.6 μM for their primaquine hybrid counterpart, **3a** (Table 1). In contrast, the parent tetraoxane (ethyl ester of **14**) revealed poor activity (EC₅₀ 17 μM), suggesting that this scaffold is not very effective against the liver stages of the parasite. Furthermore, compounds **4a–h** and **4j–l** were significantly more potent than primaquine and the 1:1 combinations of **13f–14** (ethyl ester) and primaquine-artemisinin. This is consistent with what has been

previously reported for hybrids **3** [26].

Results presented in Table 1 indicate that blocking the C-5 position of the quinoline moiety with an aryl substituent did not result in any significant loss of *in vitro* antimalarial potency of the hybrid compound. Furthermore, activity against liver stage parasites is not significantly affected by the electronic or lipophilicity properties of the substituent at C-5. Overall, the results contrast sharply with what was observed for 5-substituted 8-aminoquinolines, which were poorly active even at the highest concentration tested. For example, the 5-methylphenyl derivative, **4f**, is ca. three times more potent than its 5-methylphenyl-8-

aminoquinoline precursor, **13f** (Table 1). Interestingly, these results are in line with those reported for 5-aryl-8-aminoquinolines, which have been reported to be inactive in the exoerythrocytic mouse model [28]. Of note, primaquine is only moderately active in this assay, as the drug requires metabolic activation to display potent activity [33]. Also, hepatoma cells are metabolically less competent, compared to hepatocytes, in activating primaquine [34].

2.4. Metabolic stability

Hybrid compounds **4** and **16** underwent NADPH-dependent degradation upon incubation with rat liver microsomes, with half-lives ranging from 14 min to 2.2 h (Table 2). Most compounds displayed intermediate (0.3–0.7) or low (<0.3) predicted *in vivo* hepatic extraction ratios, E_H , representing a significant improvement in metabolic stability when compared to the primaquine counterpart **3a** ($E_H = 0.81$) [26]. No obvious metabolites were detected using the analytical conditions employed for the parent compounds.

The metabolic susceptibility of compounds **4** and **16** towards microsomes was significantly affected by the lipophilicity of substituents at C-5, as indicated by the excellent correlations between the rate of metabolism, as expressed by $\log t_{1/2}$, and the corresponding Hansch $\Sigma\pi$ values for the C-5 substituent (Fig. 3). However, no clear correlation emerged between liver schizontocidal activities and rates of metabolism. For example, hybrid compounds with low (e.g. **4c**), intermediate (e.g. **4f**), and high (e.g. **4i**) susceptibility towards rat liver microsomes were equipotent in inhibiting the growth of liver stage parasites. These results strongly suggest that liver schizontocidal activity is not dependent on metabolic activation.

The 5-bromo derivative, **4i**, presented the highest susceptibility towards the microsomes ($E_H = 0.76$). This result is not entirely surprising, as 5-fluoroprimaquine was also shown to undergo bioactivation with hepatic microsomes from several species, including rat liver microsomes. According to O'Neill et al., metabolic activation of 5-fluoroprimaquine may involve epoxidation and dehalogenation [10], a pathway also most likely available to the 5-bromo derivative **4i**. Further studies are required to identify the metabolites and to confirm their mechanisms of action.

3. Conclusions

We report that tetraoxane-8- aminoquinoline hybrids with an aryl or heteroaryl group installed at the metabolically labile C-5

Table 2
In vitro metabolism of selected hybrid compounds **4** and **16** in rat liver microsomes, and the corresponding predicted *in vivo* metabolism data.

Compd.	$t_{1/2}$ (min)	$CL_{int,invitro}$ ($\mu\text{L}/\text{min}/\text{mg}$ protein)	Predicted E_H
4a	42	33.0	0.52
4b	40	34.6	0.53
4c	129	10.7	0.26
4e	100	13.9	0.31
4f	87	15.9	0.34
4h	37	37.4	0.55
4i	14	99.0	0.76
4j	35	39.6	0.56
4k	15	92.4	0.75
4l	25	55.4	0.64
16a	42	33.0	0.52
16b	60	23.1	0.43
16c	125	11.1	0.26
16d	124	11.2	0.27
3a [26]	10	132.8	0.81

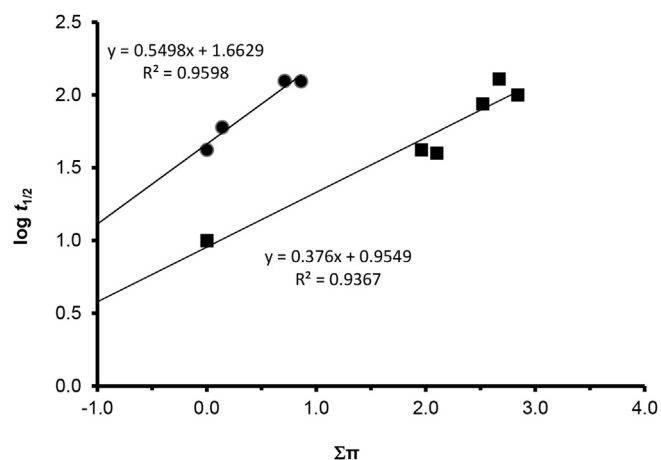


Fig. 3. Correlation between $\log t_{1/2}$ values for metabolic activation of compounds **4** (■) and **16** (●), and the corresponding Hansch $\Sigma\pi$ values for the C-5 substituents.

position of the 8-aminoquinoline moiety are efficient dual-stage antiplasmodial agents endowed with good metabolic stability. These hybrid compounds inhibited the development of intraerythrocytic forms of *P. falciparum*, with EC_{50} values ranging from the low nanomolar to low micromolar range, while displaying low cytotoxicity against mammalian cells. Compounds were also screened for activity against *P. berghei* liver stages, with the most potent compounds displaying EC_{50} values ranging from 1.1 to 4.4 μM . Analysis of SAR revealed that a linker between the endoperoxide and 8-aminoquinoline pharmacophores is crucial for dual antiplasmodial activity. In contrast to 5-aryl-8-aminoquinolines, their endoperoxide-based hybrid derivatives retain liver schizontocidal activity. In general, hybrids with aryl substituents at C-5 of the 8-aminoquinoline moiety had increased metabolic stability in microsomes when compared to their primaquine (i.e. C-5 unsubstituted) counterpart, without loss of dual stage antimalarial activity. These results also suggest that liver schizontocidal activity is not dependent on metabolic activation. Overall, this study reveals that tetraoxane-8- aminoquinoline hybrids are an attractive approach to achieve elimination of exo- and intraerythrocytic parasites, thus providing a new entry in the toolkit of multistage agents with potential utility in malaria eradication campaigns.

4. Experimental section

4.1. Chemistry

All chemicals and solvents were of analytical reagent grade and were purchased from Alfa Aesar or Sigma–Aldrich. Tetrahydrofuran was dried before use. Thin layer chromatography was performed using Merck silica gel 60F254 aluminum plates with visualization by UV light, iodine, potassium permanganate dip, and/or *p*-anisaldehyde dip. Flash column chromatography was performed using Merck silica gel 60 (230–400 mesh ASTM), eluting with various solvent mixtures and using an air aquarium pump to apply pressure. NMR spectra were collected using a Bruker 400 Ultra-Shield (400 MHz) or a Bruker 300 Avance (300 MHz) in CDCl_3 or MeOD; chemical shifts, δ , are expressed in ppm, and coupling constants, J , are expressed in Hz. Mass spectra were determined using a Micromass Quattro Micro API spectrometer equipped with a Waters 2695 HPLC module and a Waters 2996 photodiode array detector. All target compounds were determined to be >95% pure by elemental analysis (for C, H, and N), determined using a FLASH 2000 analyzer. High resolution mass spectrometry (HRMS) was

performed on a Bruker MicrOTOF equipped with ESI ion source from the Mass Spectrometry and Proteomics Unity of the University of Santiago de Compostela, Spain and a Bruker Daltonics QqTOF Impact II equipped with ESI ion source from the Laboratório de Espectrometria de Massa, Instituto Superior Técnico.

Melting points were determined using a Kofler Bock Monoscop M and are uncorrected.

The HPLC system consisted of a LichroCART 125–4 RP-18 (5 mm) analytical column on a LabChrom L7400 Merck Hitachi instrument. See [Supporting Information](#) for experimental information and data on all intermediates.

4.1.1. General procedure for the synthesis of hybrids **4a–i**

To a solution of compound **14** (0.16 mmol) in dry dichloromethane (3 mL) was added triethylamine (0.24 mmol) and TBTU (0.16 mmol). The reaction mixture was stirred for 60 min at 0 °C, under N₂ atmosphere. Then a solution of compound **13a–i** (0.16 mmol) in dry dichloromethane (2 mL) was added and, after 15 min, the mixture was allowed to warm to room temperature and react overnight. After completion of the reaction, the mixture was diluted with water and extracted with ethyl acetate. The organic phase was washed with brine, dried over anhydrous Na₂SO₄, filtered and, concentrated. Purification by flash column chromatography using ethyl acetate-hexane (4:6) as eluent gave the pure compound.

4.1.1.1. Compound 4a. Yellow solid (66% yield): mp: 75–76 °C; ¹H NMR (400 MHz, CDCl₃), δ = 8.53–8.52 (m, 1H), 7.84–7.83 (m, 1H), 7.48–7.44 (m, 2H), 7.38–7.32 (m, 3H), 7.23–7.22 (m, 1H), 6.51 (s, 1H), 6.22 (brs, 1H), 5.65 (brs, 1H), 3.83 (s, 3H), 3.76–3.74 (m, 1H), 3.39–3.22 (m, 2H), 3.20–3.01 (m, 2H), 2.20–2.09 (m, 1H), 2.03–1.53 (m, 24H), 1.36 (d, J = 6.3 Hz, 3H). ¹³C NMR (101 MHz, MeOD) δ 176.4, 155.4, 144.8, 143.9, 136.0, 133.0, 131.5, 128.9, 127.7, 126.2, 121.4, 109.9, 106.8, 93.1, 67.7, 55.6, 43.5, 38.7, 36.6, 33.4, 32.7, 27.1, 25.6, 19.5. HRMS [ESI]: m/z [M+H]⁺ calcd for C₃₈H₄₈N₃O₆: 642.3543, found: 642.3523.

4.1.1.2. Compound 4b. Yellow solid (79% yield): mp: 81–82 °C; ¹H NMR (400 MHz, CDCl₃), δ = 8.56 (dd, J = 4.1, 1.6 Hz, 1H), 7.79 (dd, J = 8.6, 1.5 Hz, 1H), 7.33–7.29 (m, 2H), 7.25 (dd, J = 8.6, 4.1 Hz, 1H), 7.19–7.14 (m, 2H), 6.51 (s, 1H), 6.29–6.19 (m, 1H), 5.61–5.53 (m, 1H), 3.85 (s, 3H), 3.82–3.72 (m, 1H), 3.46–3.23 (m, 2H), 2.21–1.65 (m, 27H), 1.38 (d, J = 6.3 Hz, 3H). ¹³C NMR (101 MHz, CDCl₃) δ 175.2, 156.0, 145.5, 144.9, 134.4, 133.9, 133.8, 132.3, 129.7, 122.5, 115.9, 115.6, 111.1, 107.7, 93.2, 57.2, 48.3, 44.8, 39.9, 37.5, 34.6, 33.7, 27.6, 26.9, 21.4. MS [ESI]: m/z [M+H]⁺ calcd for C₃₈H₄₇FN₃O₆: 660.34, found: 660.25. Anal. calcd for C₃₈H₄₆FN₃O₆: C 69.18, H 7.03, N 6.37, found: C 69.26, H 7.18, N 6.56.

4.1.1.3. Compound 4c. Yellow solid (54% yield): mp: 104–105 °C; ¹H NMR (400 MHz, MeOD), δ = 8.56–8.46 (m, 1H), 7.80–7.71 (m, 1H), 7.43 (d, J = 8.1 Hz, 2H), 7.31–7.20 (m, 3H), 6.62 (s, 1H), 4.66 (brs, 1H), 3.93–3.75 (m, 4H), 3.28–2.99 (m, 4H), 2.27–2.16 (m, 2H), 1.87–1.58 (m, 24H), 1.36 (d, J = 6.3 Hz, 3H). ¹³C NMR (101 MHz, MeOD) δ 176.4, 155.5, 145.2, 144.0, 134.8, 133.7, 133.1, 132.6, 132.0, 128.7, 127.8, 121.7, 109.9, 109.5, 106.8, 92.6, 60.2, 55.4, 43.9, 41.5, 38.5, 36.6, 33.4, 32.7, 27.1, 25.5, 19.5, 13.1. Anal. calcd for C₃₈H₄₆ClN₃O₆: C 67.49, H 6.86, N 6.21, found: C 67.44, H 6.96, N 6.18.

4.1.1.4. Compound 4d. Yellow solid (68% yield): mp: 105–107 °C; ¹H NMR (400 MHz, CDCl₃), δ = 8.53–8.54 (m, 1H), 7.79 (brs, 1H), 7.58 (d, J = 7.8 Hz, 2H), 7.27–7.25 (m, 1H), 7.20 (d, J = 8.0 Hz, 2H), 6.49 (s, 1H), 6.24 (brs, 1H), 5.56 (brs, 1H), 3.84 (s, 3H), 3.78–3.70 (m, 1H), 3.40–3.22 (m, 2H), 3.20–2.98 (m, 2H), 2.22–2.09 (m, 1H), 2.00–1.52 (m, 24H), 1.35 (d, J = 6.2 Hz, 3H). ¹³C NMR (101 MHz,

MeOD) δ 176.4, 155.4, 145.1, 144.0, 135.2, 133.4, 132.7, 130.9, 128.6, 121.7, 120.1, 110.0, 106.8, 92.6, 55.6, 43.6, 38.7, 36.6, 33.4, 32.8, 27.1, 25.6, 19.6. HRMS [ESI]: m/z [M+H]⁺ calcd for C₃₈H₄₇BrN₃O₆: 720.2648, found: 720.2619.

4.1.1.5. Compound 4e. Yellow solid (84% yield): mp: 93–95 °C; ¹H NMR (400 MHz, MeOD), δ = 8.69–8.68 (m, 1H), 7.95–7.93 (m, 1H), 7.86 (d, J = 7.9 Hz, 2H), 7.63 (d, J = 7.9 Hz, 2H), 7.44 (dd, J = 8.5, 4.0 Hz, 1H), 6.72 (s, 1H), 4.01 (s, 3H), 3.97–3.96 (m, 1H), 3.42–3.30 (m, 4H), 2.43–2.33 (m, 1H), 2.18–1.69 (m, 24H), 1.54 (d, J = 6.2 Hz, 3H). ¹³C NMR (101 MHz, MeOD) δ 176.2, 155.5, 145.3, 144.2, 140.1, 133.6, 132.9, 132.1, 128.6, 124.8, 124.8, 122.0, 110.3, 109.4, 107.0, 92.5, 60.5, 56.1, 43.7, 41.3, 39.0, 36.7, 33.8, 32.9, 27.0, 25.8, 20.1, 13.7. HRMS [ESI]: m/z [M+H]⁺ calcd for C₃₉H₄₇F₃N₃O₆: 710.3417, found: 710.3394.

4.1.1.6. Compound 4f. Yellow solid (78% yield): mp: 93–94 °C; ¹H NMR (400 MHz, MeOD), δ = 8.46–8.45 (m, 1H), 7.76–7.74 (m, 1H), 7.23–7.20 (m, 3H), 7.11 (d, J = 8.0 Hz, 2H), 6.58 (s, 1H), 5.46 (s, 1H), 3.82–3.77 (m, 4H), 3.20–3.08 (m, 4H), 2.38 (s, 3H), 2.25–2.11 (m, 1H), 2.00–1.40 (m, 24H), 1.32 (d, J = 6.3 Hz, 3H). ¹³C NMR (101 MHz, MeOD) δ 176.4, 155.4, 144.7, 143.9, 135.8, 133.8, 133.1, 132.9, 131.3, 129.0, 128.3, 121.3, 111.3, 109.9, 106.8, 93.3, 55.6, 43.5, 38.7, 36.6, 33.4, 32.7, 27.1, 25.5, 19.9, 19.4. HRMS [ESI]: m/z [M+H]⁺ calcd for C₃₉H₅₀N₃O₆: 656.3700, found: 656.3685.

4.1.1.7. Compound 4g. Yellow solid (54% yield): mp: 70–71 °C; ¹H NMR (400 MHz, CDCl₃), δ = 8.54–8.53 (m, 1H), 8.07–7.96 (m, 1H), 7.43–7.41 (m, 1H), 7.31–7.23 (m, 2H), 7.14–7.13 (m, 1H), 6.49 (s, 1H), 6.23 (brs, 1H), 5.62 (brs, 1H), 3.86 (s, 3H), 3.78–3.74 (m, 1H), 3.34–3.25 (m, 2H), 3.18–3.03 (m, 2H), 2.20–2.08 (m, 1H), 1.95–1.61 (m, 24H), 1.35 (d, J = 6.4 Hz, 3H). ¹³C NMR (101 MHz, CDCl₃) δ 174.5, 141.7, 133.2, 121.9, 115.3, 115.1, 113.5, 110.5, 107.1, 60.4, 56.6, 47.9, 44.1, 39.3, 36.9, 34.0, 33.1, 27.0, 26.3, 21.1, 20.7, 14.2. Anal. calcd for C₃₆H₄₅N₃O₇: C 68.44, H 7.18, N 6.65, found: C 68.35, H 7.28, N 6.63.

4.1.1.8. Compound 4h. Orange solid (49% yield): mp: 66–68 °C; ¹H NMR (400 MHz, CDCl₃), δ = 8.54–8.53 (m, 1H), 8.01–7.99 (m, 1H), 7.42 (dd, J = 4.7, 3.1 Hz, 1H), 7.26–7.23 (m, 2H), 7.14–7.13 (m, 1H), 6.49 (s, 1H), 6.22 (brs, 1H), 5.59 (brs, 1H), 3.86 (s, 3H), 3.75–3.74 (m, 1H), 3.33–3.26 (m, 2H), 3.15–3.04 (m, 2H), 2.17–2.08 (m, 1H), 2.03–1.51 (m, 24H), 1.35 (d, J = 6.4 Hz, 3H). ¹³C NMR (101 MHz, MeOD) δ 176.4, 156.0, 144.9, 143.9, 135.4, 133.8, 133.0, 130.6, 129.2, 123.9, 121.5, 109.9, 106.8, 93.1, 55.5, 43.5, 38.7, 37.5, 36.6, 33.3, 32.7, 27.2, 25.5, 19.4. Anal. calcd for C₃₆H₄₅N₃O₆S: C 66.74, H 7.00, N 6.49, found: C 66.52, H 6.84, N 6.33.

4.1.1.9. Compound 4i. Brown oil (63% yield); ¹H NMR (300 MHz, CDCl₃), δ = 8.47 (dd, J = 4.1, 1.6 Hz, 1H), 8.32 (dd, J = 8.6, 1.5 Hz, 1H), 7.35 (dd, J = 8.6, 4.2 Hz, 1H), 6.37 (s, 1H), 6.19–6.07 (m, 1H), 5.51–5.34 (m, 1H), 3.94 (s, 3H), 3.85–3.79 (m, 1H), 3.32–3.12 (m, 2H), 1.93–1.53 (m, 27H), 1.25 (d, J = 6.4 Hz, 3H). ¹³C NMR (75 MHz, CDCl₃) δ 171.4, 147.6, 144.9, 144.7, 134.4, 128.7, 122.9, 110.5, 107.1, 92.9, 56.9, 47.8, 44.1, 36.9, 34.3, 33.9, 33.1, 27.0, 25.5, 21.8, 19.1. HRMS [ESI]: m/z [M+H]⁺ calcd for C₃₂H₄₃BrN₃O₆: 644.2335, found: 644.2313.

4.1.2. General procedure for the synthesis of hybrids **4j–l**

To a solution of compound **14** (0.31 mmol) in dry dichloromethane (7 mL) was added triethylamine (0.5 mmol) and TBTU (0.31 mmol). The reaction mixture was stirred for 60 min at 0 °C, under N₂ atmosphere. Then a solution of compound **13j–l** (0.31 mmol) and triethylamine (0.33 mmol) in dry dichloromethane (2 mL) was added and, after 30 min, the mixture was allowed to warm to room temperature and react overnight. After

completion of the reaction, the mixture was diluted with ethyl acetate and washed with NaHCO₃. The combined organic phase was washed with brine, dried over anhydrous Na₂SO₄, filtered and concentrated. Purification by flash column chromatography using ethyl acetate-hexane (4:6) as eluent gave the pure compound.

4.1.2.1. Compound 4j. Yellow solid (88% yield); mp: 110–112 °C; ¹H RMN (300 MHz, CDCl₃) δ 8.47 (dd, J = 4.1, 1.6 Hz, 1H), 7.70 (dd, J = 8.6, 1.6 Hz, 1H), 7.25–7.19 (m, 2H), 7.18–7.13 (m, 1H), 7.12–7.03 (m, 2H), 6.43 (s, 1H), 6.32 (brs, 1H), 5.86–5.76 (m, 1H), 3.77 (s, 3H), 3.50–3.32 (m, 4H), 2.13–1.48 (m, 25H). ¹³C NMR (75 MHz, CDCl₃) δ 174.6, 163.4, 160.2, 155.4, 145.5, 144.5, 133.9, 133.2, 133.1, 131.7, 131.6, 128.9, 122.0, 115.3, 115.0, 110.6, 110.5, 107.1, 92.6, 56.6, 44.1, 41.5, 38.0, 36.9, 33.1, 29.0, 27.0. HRMS [ESI]: m/z [M+H]⁺ calcd for C₃₆H₄₃FN₃O₆: 632.3136, found: 632.3107.

4.1.2.2. Compound 4k. Yellow solid (71% yield); mp: 108–110 °C; ¹H RMN (300 MHz, CDCl₃) δ 8.54 (dd, J = 4.1, 1.5 Hz, 1H), 7.77 (dd, J = 8.6, 1.5 Hz, 1H), 7.32–7.27 (m, 2H), 7.25–7.20 (m, 1H), 7.19–7.10 (m, 2H), 6.48 (s, 1H), 6.31 (brs, 1H), 5.69–5.52 (m, 1H), 3.84 (s, 3H), 3.47–3.30 (m, 4H), 2.23–1.53 (m, 27H). ¹³C NMR (75 MHz, CDCl₃) δ 174.5, 163.4, 160.2, 155.5, 145.8, 144.4, 133.9, 133.3, 133.2, 133.1, 131.8, 131.7, 128.9, 121.9, 115.2, 115.0, 111.0, 110.4, 107.1, 93.0, 56.6, 44.2, 42.9, 39.1, 36.9, 33.1, 27.5, 27.1, 26.6. HRMS [ESI]: m/z [M+H]⁺ calcd for C₃₇H₄₅FN₃O₆: 646.3292, found: 646.3263.

4.1.2.3. Compound 4l. Yellow solid (77% yield); mp: 100–102 °C; ¹H RMN (300 MHz, CDCl₃) δ 8.46 (dd, J = 4.1, 1.6 Hz, 1H), 7.69 (dd, J = 8.6, 1.6 Hz, 1H), 7.26–7.18 (m, 2H), 7.17–7.12 (m, 1H), 7.11–7.01 (m, 2H), 6.40 (s, 1H), 6.23 (brs, 1H), 5.56–5.41 (m, 1H), 3.77 (s, 3H), 3.34–3.15 (m, 4H), 2.22–1.34 (m, 29H). ¹³C NMR (75 MHz, CDCl₃) δ 174.4, 163.4, 160.2, 155.5, 145.9, 144.4, 133.9, 133.3, 133.2, 133.1, 131.8, 131.8, 128.9, 121.9, 115.2, 115.0, 110.5, 110.2, 107.1, 92.4, 56.6, 44.2, 43.2, 39.2, 36.9, 33.1, 29.5, 28.8, 27.1, 24.5. HRMS [ESI]: m/z [M+H]⁺ calcd for C₃₈H₄₇FN₃O₆: 660.3449, found: 660.3417.

4.1.3. General procedure for the synthesis of hybrids 4m–s

To a solution of compound **15** (0.052 mmol) in dry dichloromethane (1 mL) was added the primaquine derivative **13a–c** and **13e–h** (0.057 mmol). After stirring for 1 h at room temperature under N₂ atmosphere, AcOH (0.078 mmol) and STAB (0.078 mmol) were added. After 16 h, AcOH (0.052 mmol) and STAB (0.052 mmol) were added to allow the reaction to go to completion. The mixture was diluted and basified to pH 10 with saturated aqueous NaHCO₃ and the aqueous phase was then extracted with dichloromethane and ethyl acetate. The organic phase was washed with brine, dried over anhydrous Na₂SO₄, filtered and concentrated. Purification by flash column chromatography using ethyl acetate-hexane (4:6) as eluent gave the pure compound.

4.1.3.1. Compound 4m. Yellow solid (42% yield); mp: 52–53 °C; ¹H NMR (400 MHz, MeOD), δ = 8.52–8.47 (m, 1H), 7.82 (brs, 1H), 7.80–7.74 (m, 1H), 7.46–7.38 (m, 2H), 7.37–7.29 (m, 2H), 7.28–7.21 (m, 3H), 6.61 (s, 1H), 3.90–3.82 (m, 1H), 3.80 (s, 3H), 3.16–2.93 (m, 2H), 2.79–2.67 (m, 2H), 2.57–2.49 (m, 2H), 2.04–1.49 (m, 25H), 1.36 (d, J = 6.2 Hz, 3H). ¹³C NMR (101 MHz, MeOD) δ 144.0, 136.2, 136.0, 133.2, 131.5, 127.8, 126.3, 121.5, 107.4, 93.3, 55.8, 54.0, 49.0, 36.6, 35.6, 33.8, 32.8, 27.1, 19.8. HRMS [ESI]: m/z [M+H]⁺ calcd for C₃₈H₅₀N₃O₅: 628.3750, found: 628.3727.

4.1.3.2. Compound 4n. Yellow solid (62% yield); mp: 75–77 °C; ¹H NMR (400 MHz, MeOD), δ = 8.50–8.44 (m, 1H), 7.75–7.69 (m, 1H), 7.29–7.08 (m, 5H), 6.60 (s, 1H), 3.89–3.70 (m, 4H), 3.14–2.88 (m, 2H), 2.75–2.60 (m, 2H), 2.54–2.41 (m, 2H), 2.05–1.39 (m, 25H), 1.33 (d, J = 6.2 Hz, 3H). ¹³C NMR (101 MHz, MeOD) δ 155.6, 145.0, 144.0,

133.2, 133.1, 132.8, 132.0, 129.0, 121.6, 114.5, 114.3, 109.8, 107.4, 92.8, 55.5, 53.9, 36.6, 35.6, 33.8, 32.7, 27.1, 24.7, 19.6. HRMS [ESI]: m/z [M+H]⁺ calcd for C₃₈H₄₉FN₃O₆: 646.3656, found: 646.3627.

4.1.3.3. Compound 4o. Yellow solid (78% yield); mp: 79–81 °C; ¹H NMR (400 MHz, MeOD), δ = 8.52–8.44 (m, 1H), 7.77–7.68 (m, 1H), 7.38 (d, J = 7.9 Hz, 2H), 7.29–7.16 (m, 3H), 6.60 (s, 1H), 3.88–3.80 (m, 1H), 3.78 (s, 3H), 3.12–2.90 (m, 2H), 2.83–2.72 (m, 2H), 2.60–2.50 (m, 2H), 2.26–2.17 (m, 1H), 2.01–1.48 (m, 24H), 1.32 (d, J = 6.2 Hz, 3H). ¹³C NMR (101 MHz, MeOD) δ 155.5, 145.2, 144.1, 134.7, 133.7, 133.0, 132.6, 132.1, 128.7, 127.8, 121.7, 109.9, 107.2, 92.7, 55.5, 53.4, 36.5, 35.2, 33.6, 32.7, 27.1, 24.1, 19.6. Anal. calcd for C₃₈H₄₈ClN₃O₅: C 68.92, H 7.31, N 6.34, found: C 68.63, H 7.31, N 6.21.

4.1.3.4. Compound 4p. Yellow solid (74% yield); mp: 73–74 °C; ¹H NMR (400 MHz, CDCl₃), δ = 8.60–8.52 (m, 1H), 7.83–7.76 (m, 1H), 7.75–7.69 (m, 2H), 7.53–7.43 (m, 2H), 7.33–7.24 (m, 1H), 7.22–7.15 (m, 1H), 6.52 (s, 1H), 6.40–6.26 (m, 1H), 3.87 (s, 3H), 3.82–3.71 (m, 1H), 3.27–2.99 (m, 2H), 2.80–2.67 (m, 2H), 2.58–2.47 (m, 2H), 2.13–1.48 (m, 25H), 1.39 (d, J = 6.2 Hz, 3H). ¹³C NMR (101 MHz, CDCl₃) δ 155.4, 148.9, 145.4, 144.4, 140.1, 133.9, 132.7, 132.1, 129.0, 128.6, 128.2, 125.3, 125.1, 125.0, 122.1, 110.4, 108.0, 92.3, 56.5, 55.0, 49.9, 48.1, 39.1, 36.9, 36.7, 34.6, 33.1, 29.7, 27.0, 26.2, 20.7. Anal. calcd for C₃₉H₄₈F₃N₃O₅: C 67.32, H 6.95, N 6.04, found: C 67.10, H 6.85, N 6.13.

4.1.3.5. Compound 4q. Yellow solid (68% yield); mp: 75–76 °C; ¹H NMR (400 MHz, MeOD), δ = 8.49–8.42 (m, 1H), 7.79–7.70 (m, 1H), 7.28–7.17 (m, 3H), 7.14–7.06 (m, 2H), 6.59 (s, 1H), 3.87–3.78 (m, 1H), 3.76 (s, 3H), 3.13–2.91 (m, 2H), 2.74–2.57 (m, 2H), 2.50–2.41 (m, 2H), 2.37 (s, 3H), 2.02–1.47 (m, 25H), 1.32 (d, J = 6.3 Hz, 3H). ¹³C NMR (101 MHz, MeOD) δ 155.4, 144.7, 143.9, 135.9, 133.2, 132.9, 131.3, 129.1, 128.4, 121.4, 111.4, 109.8, 107.4, 93.3, 55.6, 54.1, 49.1, 36.6, 35.8, 33.9, 32.7, 27.1, 24.8, 19.9, 19.7. Anal. calcd for C₃₉H₅₁N₃O₅: C 72.98, H 8.01, N 6.55, found: C 73.07, H 7.98, N 6.62.

4.1.3.6. Compound 4r. Yellow solid (57% yield); mp: 62–64 °C; ¹H NMR (400 MHz, MeOD) δ 8.57–8.50 (m, 1H), 8.21–8.11 (m, 1H), 7.68–7.59 (m, 1H), 7.58–7.50 (m, 1H), 7.41–7.29 (m, 1H), 7.27–7.03 (m, 1H), 6.64 (s, 1H), 6.53 (s, 1H), 3.94–3.77 (m, 4H), 3.20–2.95 (m, 2H), 2.82–2.71 (m, 2H), 2.59–2.50 (m, 2H), 2.09–1.48 (m, 25H), 1.38 (d, J = 6.3 Hz, 3H). ¹³C NMR (101 MHz, MeOD) δ 156.2, 144.8, 144.0, 142.1, 141.6, 133.1, 129.1, 121.6, 113.2, 109.8, 107.3, 93.1, 55.6, 53.7, 36.6, 35.5, 33.7, 32.7, 29.4, 27.1, 24.5, 19.6. Anal. calcd for C₃₆H₄₇N₃O₆: C 69.99, H 7.67, N 6.80, found: C 69.79, H 7.74, N 6.77.

4.1.3.7. Compound 4s. Yellow solid (76% yield); mp: 66–67 °C; ¹H NMR (400 MHz, MeOD) δ = 8.55–8.45 (m, 1H), 7.99–7.90 (m, 1H), 7.51–7.40 (m, 1H), 7.34–7.25 (m, 1H), 7.24–7.19 (m, 1H), 7.12–7.03 (m, 1H), 6.59 (s, 1H), 3.82 (s, 3H), 3.17–2.92 (m, 2H), 2.79–2.62 (m, 2H), 2.57–2.42 (m, 2H), 2.34–2.10 (m, 1H), 2.07–1.41 (m, 25H), 1.36 (d, J = 6.3 Hz, 3H). ¹³C NMR (101 MHz, MeOD) δ 156.0, 144.8, 144.0, 135.4, 133.8, 133.2, 130.6, 129.3, 123.9, 121.6, 109.9, 107.4, 93.2, 55.7, 54.0, 49.0, 36.6, 35.7, 33.8, 32.8, 32.7, 27.1, 24.8, 19.8. HRMS [ESI]: m/z [M+H]⁺ calcd for C₃₆H₄₈N₃O₅S: 634.3315, found: 634.3291.

4.1.4. General procedure for the synthesis of hybrids 16a–d

To a solution of compound **14** (0.25 mmol) in dry dichloromethane (5.62 mL) stirring at room temperature under N₂ atmosphere, was added ethyl chloroformate (0.28 mmol) and dry triethylamine (0.38 mmol). Product formation was monitored by thin layer chromatography and after 1 h, compounds **5a–d** (0.25 mmol) were added to the reaction mixture which was then stirred at 60 °C. After about 7 h, a saturated solution of sodium hydrogenocarbonate was added to the reaction and the mixture was

then extracted with dichloromethane. The organic phases were combined, dried over anhydrous Na₂SO₄, filtered and, concentrated. Purification by flash chromatography using ethyl acetate-hexane (4:6) as eluent gave the pure compound.

4.1.4.1. Compound 16a. Yellow solid (58% yield); mp: 184–186 °C; ¹H NMR (400 MHz, CDCl₃) δ 10.10 (s, 1H), 8.85 (s, 1H), 8.64 (d, *J* = 2.8 Hz, 1H), 7.89 (d, *J* = 8.6 Hz, 1H), 7.49 (t, *J* = 7.3 Hz, 2H), 7.41 (t, *J* = 7.3 Hz, 1H), 7.33 (d, *J* = 8.0 Hz, 2H), 7.31–7.28 (m, 1H), 3.91 (s, 3H), 3.20 (s, 2H), 2.64 (t, *J* = 10.7 Hz, 1H), 2.25–1.55 (m, 25H). ¹³C NMR (101 MHz, CDCl₃) δ 173.9, 154.7, 146.0, 135.5, 131.7, 128.7, 127.7, 122.4, 119.1, 111.0, 107.6, 57.0, 45.8, 37.4, 33.6, 27.5. HRMS [ESI]: *m/z* [M+H]⁺ calcd for C₃₃H₃₇N₂O₆: 557.2652, found: 557.2653.

4.1.4.2. Compound 16b. Yellow solid (52% yield); mp: 204–206 °C; ¹H NMR (400 MHz, CDCl₃) δ 10.09 (s, 1H), 8.84 (s, 1H), 8.64 (d, *J* = 3.6 Hz, 1H), 7.85 (d, *J* = 8.4 Hz, 1H), 7.34–7.27 (m, 3H), 7.17 (t, *J* = 8.6 Hz, 2H), 3.91 (s, 3H), 3.21 (s, 2H), 2.63 (t, *J* = 7.1 Hz, 1H), 2.20–1.61 (m, 24H); ¹³C NMR (101 MHz, CDCl₃) δ 173.7, 163.6, 161.2, 154.9, 145.8, 135.5, 133.7, 133.0, 130.9, 128.6, 122.5, 117.7, 115.6, 110.7, 107.3, 56.8, 45.7, 37.1, 33.4, 30.2, 27.3. HRMS [ESI]: *m/z* [M+H]⁺ calcd for C₃₃H₃₆FN₂O₆: 575.2557, found: 575.2552.

4.1.4.3. Compound 16c. Yellow solid (51% yield); mp: 208–210 °C; ¹H NMR (400 MHz, CDCl₃) δ 10.09 (s, 1H), 8.84 (s, 1H), 8.64 (d, *J* = 3.0 Hz, 1H), 7.86 (d, *J* = 8.5 Hz, 1H), 7.46 (d, *J* = 8.2 Hz, 2H), 7.32 (dd, *J* = 8.6, 4.1 Hz, 1H), 7.27 (d, *J* = 7.6 Hz, 3H), 3.91 (s, 3H), 3.20 (s, 1H), 2.63 (t, *J* = 10.9 Hz, 1H), 2.23–1.54 (m, 26H). ¹³C NMR (101 MHz, CDCl₃) δ 173.6, 154.6, 145.8, 135.6, 133.6, 133.4, 132.8, 128.7, 128.0, 122.2, 117.3, 110.7, 107.2, 104.5, 56.7, 45.5, 37.1, 33.3, 29.9, 27.2. HRMS [ESI]: *m/z* [M+H]⁺ calcd for C₃₃H₃₆ClN₂O₆: 591.2262, found: 591.2260.

4.1.4.4. Compound 16d. Yellow solid (52% yield); mp: 212–214 °C; ¹H NMR (400 MHz, CDCl₃) δ 10.09 (s, 1H), 8.83 (s, 1H), 8.64 (d, *J* = 2.8 Hz, 1H), 7.86 (d, *J* = 8.5 Hz, 1H), 7.61 (d, *J* = 8.2 Hz, 2H), 7.32 (dd, *J* = 8.6, 4.1 Hz, 1H), 7.21 (d, *J* = 8.3 Hz, 2H), 3.90 (s, 3H), 3.20 (s, 1H), 2.63 (t, *J* = 10.9 Hz, 1H), 2.17–1.56 (m, 28H). ¹³C NMR (101 MHz, CDCl₃) δ 173.6, 154.4, 145.8, 135.5, 134.1, 133.1, 131.6, 128.0, 122.3, 121.6, 117.2, 110.7, 107.2, 104.4, 56.7, 45.5, 37.1, 33.3, 29.9, 27.2, 19.0. HRMS [ESI]: *m/z* [M+H]⁺ calcd for C₃₃H₃₆BrN₂O₆: 635.1757, found: 635.1747.

4.2. Biology

4.2.1. Activity against erythrocytic-stage *P. falciparum*

Human erythrocytes infected with about 1% parasitemia of ring-stage W2 strain *P. falciparum* synchronized with 5% sorbitol were incubated with test compounds in 96-well plates at 37 °C for 48 h in RPMI-1640 medium, supplemented with 25 mM 4-(2-hydroxyethyl)-1-piperazineethanesulfonic acid (HEPES) pH 7.4, 10% heat inactivated human serum (or 0.5% Albumax, 2% human serum), and 100 μM hypoxanthine under an atmosphere of 3% O₂, 5% CO₂, and 91% N₂. After 48 h, the cells were fixed in 2% formaldehyde in phosphate-buffered saline (PBS) and transferred into PBS with 100 mM NH₄Cl, 0.1% Triton X-100, 1 nM YOYO-1, and infected erythrocytes were counted in a flow cytometer (FACSort, Beckton Dickinson; EX 488 nm, EM 520 nm). Values of IC₅₀ based on comparisons with untreated control cultures were calculated by using GraphPad PRISM software. Two independent experiments were performed, each with four replicates for each of the experimental conditions.

4.2.2. Activity against *P. berghei* liver stages

Inhibition of hepatic infection by test compounds was

determined by measuring the luminescence intensity in Huh-7 cells infected with a firefly luciferase-expressing *P. berghei* line as previously described [35]. Briefly, Huh-7 cells, a human hepatoma cell line, were cultured in RPMI-1640 medium supplemented with 10% (v/v) fetal bovine serum, 1% (v/v) nonessential amino acids, 1% (v/v) penicillin/streptomycin, 1% (v/v) glutamine, and 10 mM HEPES, pH 7, and maintained at 37 °C with 5% CO₂. For infection assays, Huh-7 cells (1.0 × 10⁴ per well) were seeded in 96-well plates the day before drug treatment and infection. The medium was replaced by medium containing the appropriate concentration of each compound approximately 1 h prior to infection with sporozoites freshly obtained through disruption of salivary glands of infected female *Anopheles stephensi* mosquitoes. In control wells, the compounds' vehicle (DMSO) was added in an amount equivalent to that present in the highest drug concentration employed. Sporozoite addition was followed by centrifugation at 1700 g for 5 min. Parasite infection load was measured 48 h after infection by a bioluminescence assay (Biotium, Hayward, CA). The effect of the compounds on the viability of Huh-7 cells was assessed by the AlamarBlue assay (Life) using the manufacturer's protocol. All compounds were initially screened at 1 and 10 μM and compounds selected for EC₅₀ determination were additionally assessed at various concentrations determined on the basis of the initial activity screen. Nonlinear regression analysis was employed to fit the normalized results of the dose-response curves, and EC₅₀ values were determined using GraphPad Prism V 5.0.

4.2.3. Metabolism studies

Compounds **4** and **16** were incubated with a reaction mixture consisting of rat liver microsomal protein (20 μL of a 20 mg mL⁻¹ solution) in 50 mM PBS (160 μL), water (570 μL), NADPH regenerating system solution A (40 μL, containing 31 mM NADP⁺, 66 mM glucose 6-phosphatase, and 0.67 mM MgCl₂), and NADPH regenerating system solution B (8 μL, containing 40 U mL⁻¹ glucose-6-phosphate dehydrogenase in 5 mM sodium citrate). After preincubation at 37 °C for 5 min, enzyme reactions were initiated by adding the parent solution of the drug (2 μL, 1 mM) in DMSO. Samples were aliquoted (80 μL) at various time points and stopped by protein precipitation through addition of an equal volume of ice-cold acetonitrile. The mixtures were centrifuged at 10,000 g for 10 min at room temperature. The supernatants were immediately analyzed, and the remaining parent drug versus time was quantified by HPLC. The HPLC system consisted of a LichroCART 125-4 RP-18 (5 μm) analytical column on a LabChrom L7400 Merck Hitachi instrument, with a mixture of methanol/water (85:15) as eluent at a flow rate of 1 mL min⁻¹. HPLC detection was at the maximum of absorbance of compounds **4** and **16** (λ = 266 nm). The corresponding half-life values were determined in triplicate.

4.2.4. Cytotoxicity assays

Colorectal adenocarcinoma CaCo-2 cells (ATCC) were grown in RPMI-1640 medium supplemented with 10% fetal bovine serum (FBS) and antibiotic antimycotic solution (A5955, Sigma) at 37 °C in a humidified 5% CO₂ atmosphere.

CaCo-2 cells were seeded on 96-well-plates and cultured until reaching confluence. Stock solutions of the compounds were diluted with the cell culture medium and added to the confluent cells for 72 h (percentage of organic solvent ≤ 1%). After this period, medium was removed from the plates and cells were washed with PBS. Viability was determined using neutral red as described elsewhere [36]. Each experimental condition was done in triplicate. CC₅₀ values were determined using GraphPad Prism software.

Acknowledgements

This work was supported by Fundação para a Ciência e Tecnologia (FCT), Portugal, through grants Pest-OE/SAU/UI4013/2014, REDE/1501/REM/2005, ROTEIRO/0028/2013, LISBOA-01-0145-FEDER-022125 and PTDC/SAU-FAR/118459/2010, and fellowships SFRH/BPD/100645/2014 (RC) and Investigator FCT (MP).

Appendix A. Supplementary data

Supplementary data related to this article can be found at <https://doi.org/10.1016/j.ejmech.2018.02.048>.

References

- [1] WHO, World Malaria Report, 2015.
- [2] M. Prudencio, M.M. Mota, A.M. Mendes, A toolbox to study liver stage malaria, *Trends Parasitol.* 27 (2011) 565–574.
- [3] T. Rodrigues, M. Prudencio, R. Moreira, M.M. Mota, F. Lopes, Targeting the liver stage of malaria parasites: a yet unmet goal, *J. Med. Chem.* 55 (2012) 995–1012.
- [4] T.N. Wells, J.N. Burrows, J.K. Baird, Targeting the hypnozoite reservoir of *Plasmodium vivax*: the hidden obstacle to malaria elimination, *Trends Parasitol.* 26 (2010) 145–151.
- [5] S.K. Nilsson, L.M. Childs, C. Buckee, M. Marti, Targeting human transmission biology for malaria elimination, *PLoS Pathog.* 11 (2015).
- [6] T.N.C. Wells, R.H. van Huijsduijnen, W.C. Van Voorhis, Malaria medicines: a glass half full? *Nat. Rev. Drug Discov.* 14 (2015) 424–442.
- [7] J.N. Burrows, S. Duparc, W.E. Gutteridge, R.H. van Huijsduijnen, W. Kaszubska, F. Macintyre, S. Mazzuri, J.J. Mohrle, T.N.C. Wells, New developments in anti-malarial target candidate and product profiles, *Malaria J.* 16 (2017).
- [8] P.L. Alonso, A. Djimde, P. Krensner, A. Magill, J. Milman, J. Najera, C.V. Plowe, R. Rabinovich, T. Wells, S. Yeung, M.C.G. drugs, a research agenda for malaria eradication: drugs, *PLoS Med.* 8 (2011).
- [9] N. Vale, R. Moreira, P. Gomes, Primaquine revisited six decades after its discovery, *Eur. J. Med. Chem.* 44 (2009) 937–953.
- [10] P.M. O'Neill, M.D. Tingle, R. Mahmud, R.C. Storr, S.A. Ward, B.K. Park, The effect of fluorine substitution on the haemotoxicity of primaquine, *Bioorg. Med. Chem. Lett.* 5 (1995) 2309–2314.
- [11] A. Martinelli, R. Moreira, P.V.L. Cravo, Malaria combination therapies: advantages and shortcomings, *Mini Rev. Med. Chem.* 8 (2008) 201–212.
- [12] E.A. Ashley, M. Dhorja, R.M. Fairhurst, C. Amaratunga, P. Lim, S. Suon, S. Sreng, J.M. Anderson, S. Mao, B. Sam, C. Sopha, C.M. Chuor, C. Nguon, S. Sovannaroth, S. Pukrittayakamee, P. Jittamala, K. Chotivanich, K. Chutasmit, C. Suchatsoonthorn, R. Runcharoen, T.T. Hien, N.T. Thuy-Nhien, N.V. Thanh, N.H. Phu, Y. Htut, K.T. Han, K.H. Aye, O.A. Mokuolu, R.R. Olaosebikan, O.O. Folaranmi, M. Mayxay, M. Khanthavong, B. Hongvanthong, P.N. Newton, M.A. Onyamboko, C.I. Fanello, A.K. Tshefu, N. Mishra, N. Valecha, A.P. Phyto, F. Nosten, P. Yi, R. Tripura, S. Borrmann, M. Bashraheil, J. Peshu, M.A. Faiz, A. Ghose, M.A. Hossain, R. Samad, M.R. Rahman, M.M. Hasan, A. Islam, O. Miotto, R. Amato, B. MacLinnis, J. Stalker, D.P. Kwiatkowski, Z. Bozdech, A. Jeeyapant, P.Y. Cheah, T. Sakulthaew, J. Chalk, B. Intharabut, K. Silamut, S.J. Lee, B. Vihokhern, C. Kunasol, M. Imwong, J. Tarning, W.J. Taylor, S. Yeung, C.J. Woodrow, J.A. Flegg, D. Das, J. Smith, M. Venkatesan, C.V. Plowe, K. Stepniewska, P.J. Guerin, A.M. Dondorp, N.P. Day, N.J. White, Spread of artemisinin resistance in *Plasmodium falciparum* malaria, *New Engl. J. Med.* 371 (2014) 411–423.
- [13] A.M. Dondorp, F. Nosten, P. Yi, D. Das, A.P. Phyto, J. Tarning, K.M. Lwin, F. Ariey, W. Hanphitakpong, S.J. Lee, P. Ringwald, K. Silamut, M. Imwong, K. Chotivanich, P. Lim, T. Herdman, S.S. An, S. Yeung, P. Singhasivanon, N.P.J. Day, N. Lindegardh, D. Socheat, N.J. White, Artemisinin resistance in *Plasmodium falciparum* malaria, *New Engl. J. Med.* 361 (2009) 455–467.
- [14] A.M. Dondorp, S. Yeung, L. White, C. Nguon, N.P.J. Day, D. Socheat, L. von Seidlein, Artemisinin resistance: current status and scenarios for containment, *Nat. Rev. Microbiol.* 8 (2010) 272–280.
- [15] A. Mbengue, S. Bhattacharjee, T. Pandharkar, H.N. Liu, G. Estiu, R.V. Stahelin, S.S. Rizk, D.L. Njimoh, Y. Ryan, K. Chotivanich, C. Nguon, M. Ghorbal, J.J. Lopez-Rubio, M. Pfrender, S. Emrich, N. Mohandas, A.M. Dondorp, O. Wiest, K. Haldar, A molecular mechanism of artemisinin resistance in *Plasmodium falciparum* malaria, *Nature* 520 (2015) 683–687.
- [16] R.M. Fairhurst, A.M. Dondorp, Artemisinin-resistant *Plasmodium falciparum* malaria, *Microbiol. Spectr.* 4 (2016).
- [17] B. Meunier, Hybrid molecules with a dual mode of action: dream or reality? *Accounts Chem. Res.* 41 (2008) 69–77.
- [18] R. Capela, R. Oliveira, L.M. Goncalves, A. Domingos, J. Gut, P.J. Rosenthal, F. Lopes, R. Moreira, Artemisinin-dipeptidyl vinyl sulfone hybrid molecules: design, synthesis and preliminary SAR for antiparasitodal activity and falcipain-2 inhibition, *Bioorg. Med. Chem. Lett.* 19 (2009) 3229–3232.
- [19] H. Kaur, M. Machado, C. de Kock, P. Smith, K. Chibale, M. Prudencio, K. Singh, Primaquine-pyrimidine hybrids: synthesis and dual-stage antiparasitodal activity, *Eur. J. Med. Chem.* 101 (2015) 266–273.
- [20] R. Oliveira, R.C. Guedes, P. Meireles, I.S. Albuquerque, L.M. Goncalves, E. Pires, M.R. Bronze, J. Gut, P.J. Rosenthal, M. Prudencio, R. Moreira, P.M. O'Neill, F. Lopes, Tetraoxane-pyrimidine nitrile hybrids as dual stage antimalarials, *J. Med. Chem.* 57 (2014) 4916–4923.
- [21] R. Oliveira, D. Miranda, J. Magalhaes, R. Capela, M.J. Perry, P.M. O'Neill, R. Moreira, F. Lopes, From hybrid compounds to targeted drug delivery in antimalarial therapy, *Bioorg. Med. Chem.* 23 (2015) 5120–5130.
- [22] R. Oliveira, A.S. Newton, R.C. Guedes, D. Miranda, R.K. Amewu, A. Srivastava, J. Gut, P.J. Rosenthal, P.M. O'Neill, S.A. Ward, F. Lopes, R. Moreira, An endoperoxide-based hybrid approach to deliver falcipain inhibitors inside malaria parasites, *ChemMedChem* 8 (2013) 1528–1536.
- [23] C.J.A. Ribeiro, M. Espadinha, M. Machado, J. Gut, L.M. Goncalves, P.J. Rosenthal, M. Prudencio, R. Moreira, M.M.M. Santos, Novel squaramides with in vitro liver stage antiparasitodal activity, *Bioorg. Med. Chem.* 24 (2016) 1786–1792.
- [24] P.L. Alonso, G. Brown, M. Arevalo-Herrera, F. Binka, C. Chitnis, F. Collins, O.K. Doumbo, B. Greenwood, B.F. Hall, M.M. Levine, K. Mendis, R.D. Newman, C.V. Plowe, M.H. Rodriguez, R. Sinden, L. Slutsker, M. Tanner, A research agenda to underpin malaria eradication, *PLoS Med.* 8 (2011).
- [25] R. Capela, G.G. Cabal, P.J. Rosenthal, J. Gut, M.M. Mota, R. Moreira, F. Lopes, M. Prudencio, Design and evaluation of primaquine-artemisinin hybrids as a multistage antimalarial strategy, *Antimicrob. Agents Ch.* 55 (2011) 4698–4706.
- [26] D. Miranda, R. Capela, I.S. Albuquerque, P. Meireles, I. Paiva, F. Nogueira, R. Amewu, J. Gut, P.J. Rosenthal, R. Oliveira, M.M. Mota, R. Moreira, F. Marti, M. Prudencio, P.M. O'Neill, F. Lopes, Novel endoperoxide-based transmission-blocking antimalarials with liver- and blood-schizontocidal activities, *ACS Med. Chem. Lett.* 5 (2014) 108–112.
- [27] J. Vasquezvivar, O. Augusto, Hydroxylated metabolites of the antimalarial drug primaquine - oxidation and redox cycling, *J. Biol. Chem.* 267 (1992) 6848–6854.
- [28] H. Shiraki, M.P. Kozar, V. Melendez, T.H. Hudson, C. Ohrt, A.J. Magill, A.J. Lin, Antimalarial activity of novel 5-Aryl-8-aminoquinoline derivatives, *J. Med. Chem.* 54 (2011) 131–142.
- [29] E.H. Chen, A.J. Saggiomo, K. Tanabe, B.L. Verma, E.A. Nodiff, Modifications of primaquine as antimalarials .1. 5-phenoxy derivatives of primaquine, *J. Med. Chem.* 20 (1977) 1107–1109.
- [30] M.J. Portela, R. Moreira, E. Valente, L. Constantino, J. Iley, J. Pinto, R. Rosa, P. Cravo, V.E. do Rosario, Dipeptide derivatives of primaquine as transmission-blocking antimalarials: effect of aliphatic side-chain acylation on the gametocytocidal activity and on the formation of carboxyprimaquine in rat liver homogenates, *Pharm. Res.* 16 (1999) 949–955.
- [31] R.C. Elderfield, H.E. Mertel, R.T. Mitch, I.M. Wempen, E. Werble, Synthesis of primaquine and certain of its analogs, *J. Am. Chem. Soc.* 77 (1955) 4816–4819.
- [32] C. Hansch, A. Leo, R.W. Taft, A survey of hammett substituent constants and resonance and field parameters, *Chem. Rev.* 91 (1991) 165–195.
- [33] B.S. Pybus, J.C. Sousa, X.N. Jin, J.A. Ferguson, R.E. Christian, R. Barnhart, C. Vuong, R.J. Sciotti, G.A. Reichard, M.P. Kozar, L.A. Walker, C. Ohrt, V. Melendez, CYP450 phenotyping and accurate mass identification of metabolites of the 8-aminoquinoline, anti-malarial drug primaquine, *Malaria J.* 11 (2012).
- [34] S. March, S. Ng, S. Velmurugan, A. Galstian, J. Shan, David J. Logan, Anne E. Carpenter, D. Thomas, B. Kim Lee Sim, Maria M. Mota, Stephen L. Hoffman, Sangeeta N. Bhatia, A microscale human liver platform that supports the hepatic stages of *Plasmodium falciparum* and vivax, *Cell Host Microbe* 14 (2013) 104–115.
- [35] M. Machado, M. Sanches-Vaz, J.P. Cruz, A.M. Mendes, M. Prudencio, Inhibition of plasmodium hepatic infection by antiretroviral compounds, *Front. Cell. Infect. Mi.* 7 (2017).
- [36] C.A.B. Rodrigues, R.F.M. Frade, I.S. Albuquerque, M.J. Perry, J. Gut, M. Machado, P.J. Rosenthal, M. Prudencio, C.A.M. Afonso, R. Moreira, Targeting the erythrocytic and liver stages of malaria parasites with s-triazine-based hybrids, *Chem. Med. Chem* 10 (2015) 883–890.